Genes & Diseases (2022) 9, 562–575

Available online at www.sciencedirect.com

ScienceDirect

journal homepage: http://ees.elsevier.com/gendis/default.asp

FULL LENGTH ARTICLE

Protein phosphatase 6 (Pp6) is crucial for regulatory T cell function and stability in autoimmunity

Wei Cai [a,1], Junxun Zhang [a,1], Hong Zhou [a], Xiangxiao Li [b], Fangzhou Lou [a], Yang Sun [a], Zhenyao Xu [a], Jing Bai [a], Qianqian Yin [a], Zhikai Wang [a], Libo Sun [a], Xiaojie Cai [a], Sibei Tang [a], Yue Wu [a], Li Fan [a], Hong Wang [a], Honglin Wang [a,], Qun Li [b,*]**

[a] *Department of Immunology and Microbiology, Shanghai Institute of Immunology, Key Laboratory of Cell Differentiation and Apoptosis of Chinese Ministry of Education, Institute of Translational Medicine, Shanghai General Hospital, Shanghai Jiao Tong University School of Medicine (SJTU-SM), Shanghai 200025, PR China*

[b] *The Department of Cardiovascular Medicine, State Key Laboratory of Medical Genomics, Shanghai Key Laboratory of Hypertension, Ruijin Hospital, Shanghai Institute of Hypertension, Shanghai Jiao Tong University School of Medicine, Shanghai 200025, PR China*

Received 3 June 2021; received in revised form 26 July 2021; accepted 27 July 2021
Available online 17 August 2021

KEYWORDS
Akt;
DNA methyltransferase 1 (Dnmt1);
FoxP3;
Protein phosphatase 6 (Pp6);

Abstract Regulatory T (T_{reg}) cells constitute a dynamic population that is critical in autoimmunity. T_{reg} cell therapies for autoimmune diseases are mainly focused on enhancing their suppressive activities. However, recent studies demonstrated that certain inflammatory conditions induce T_{reg} cell instability with diminished FoxP3 expression and convert them into pathogenic effector cells. Therefore, the identification of novel targets crucial to both T_{reg} cell function and plasticity is of vital importance to the development of therapeutic approaches in autoimmunity. In this study, we found that conditional *Pp6* knockout (cKO) in T_{reg} cells led to spontaneous autoinflammation, immune cell activation, and diminished levels of FoxP3 in

Abbreviations: FoxP3, Forkhead box protein P3; WT, wild type; EAE, experimental allergic encephalomyelitis; TCR, T cell receptor; CTV, CellTrace Violet; Rag1, recombination-activating protein 1; TSDR, T_{reg}-specific demethylated region.

* Corresponding author. The Department of Cardiovascular Medicine, Shanghai Key Laboratory of Hypertension Ruijin Hospital, Shanghai Institute of Hypertension Shanghai Jiao Tong University School of Medicine (SJTU-SM), Shanghai 200025, PR China.
** Corresponding author. Shanghai Institute of Immunology, Shanghai Jiao Tong University School of Medicine (SJTU-SM), 280 Chongqing South Road, Shanghai 200025, PR China. Fax: +86 21 64660996.
E-mail addresses: honglin.wang@sjtu.edu.cn (H. Wang), liqun@sibs.ac.cn (Q. Li).
Peer review under responsibility of Chongqing Medical University.
[1] These authors contributed equally to this work.

https://doi.org/10.1016/j.gendis.2021.07.005

Regulatory T (T_{reg}) cells;
Stability

$CD4^+$ T cells in mice. Loss of Pp6 in T_{reg} cells exacerbated two classical mouse models of T_{reg}-related autoinflammation. Mechanistically, Pp6 deficiency increased CpG motif methylation of the *FoxP3* locus by dephosphorylating Dnmt1 and enhancing Akt phosphorylation at Ser473/Thr308, leading to impaired *FoxP3* expression in T_{reg} cells. In summary, our study proposes Pp6 as a critical positive regulator of FoxP3 that acts by decreasing DNA methylation of the FoxP3 gene enhancer and inhibiting Akt signaling, thus maintaining T_{reg} cell stability and preventing autoimmune diseases.

Introduction

Recent studies have reported that $FoxP3^+$ regulatory T (T_{reg}) cells are not a terminally differentiated cell population with a fixed phenotype; they display some degree of plasticity and/or instability under certain inflammatory conditions.[1] Although the functional stability of T_{reg} cells is a controversial issue, some groups have observed that under specific inflammatory conditions, natural and induced regulatory T (iT_{reg}) cells lose FoxP3 expression and acquire a pathogenic phenotype with the expression of pro-inflammatory cytokines, becoming so-called "exFoxP3" T_{reg} cells.[2,3] FoxP3 is a key marker for T_{reg} cells, and its stable expression is required for T_{reg} cell maintenance and immunosuppression.[4] Loss of FoxP3 in T_{reg} cells partially causes autoimmune diseases in mice and humans.[5,6] Genetic mutation of FoxP3 leads to the scurfy phenotype in mice, which includes fatal autoimmunity.[7] The mutation of human FoxP3 causes immune dysregulation, polyendocrinopathy, enteropathy, and X-linked syndrome (IPEX).[8]

Protein phosphatase 6 (Pp6) belongs to the serine/threonine protein phosphatase family.[9] *Pp6*-specific deletion in T_{reg} cells led to marked impairment of T_{reg} cell induction and increased Ang II-induced blood pressure elevation in mice.[10] However, the exact function of Pp6 in T_{reg} cells remains elusive. In this study, we found that conditional *Pp6* knockout (cKO) in T_{reg} cells led to diminished levels of FoxP3, which inspired us to explore the underlying mechanism.

Recent studies revealed that FoxP3 stability depends on the demethylation of the CpG motif in the FoxP3 locus, especially in the T_{reg} cell-specific demethylated region (TSDR).[11,12] Three kinds of DNA methyltransferase (Dnmt) enzymes are responsible for DNA methylation: Dnmt1, Dnmt3a, and Dnmt3b.[13] In mice, Dnmt1 deficiency in T_{reg} cells weakens their suppressive function, while Dnmt3a deficiency does not, suggesting that Dnmt1 is critical to T_{reg} cells.[14] Upon TCR signaling, Dnmt1 is upregulated to mediate FoxP3 expression by enhancing CpG methylation.[15] T_{reg} cells in patients with abdominal arterial aneurysm, a disease that shares many features with autoimmune diseases, have a significantly higher DNA methylation rate of Dnmt1 levels than the control group.[16] Elevated methylation levels of T_{reg} cell-conserved noncoding sequences in the *FoxP3* locus abrogate FoxP3 expression, leading to severe autoimmune disease.[17] However, the dynamic modulation of CpG motif methylation and activity control of Dnmt in T_{reg} cells remain elusive. Here, we report that Pp6 could bind and dephosphorylate Dnmt1, hence decreasing CpG motif methylation at the FoxP3 locus.

FoxP3 is negatively controlled by the PI3K/Akt pathway, which is a critical inhibitory signal restraining FoxP3 expression in T_{reg} cells.[37] Akt hyperactivation contributes to T_{reg} cell reduction and plasticity.[18] Interestingly, several phosphatases restrict the PI3K/Akt cascade by dephosphorylating key proteins. Protein phosphatase 2A (PP2A) mainly reduces mTOC1 activity by dephosphorylating S6 protein, with a negligible effect on phosphorylation of Akt at Ser473 and Thr308 in mouse $CD4^+$ T cells.[19,20] Conditional knockdown of *Pp6* in T cells activates TCR terminal signals, such as MAPKs, AKT, and NF-κB, leading to enhanced T cell activation and a decreased proportion of T_{reg} cells in $Pp6^{fl/fl}$-Lck^{cre} mice.[24] However, whether Pp6 modulates the phosphorylation of Akt at *Ser473/Thr308* and FoxP3 expression in T_{reg} cells remain unexplored.

In view of the known Pp6 regulation of T_{reg} cells and FoxP3 expression, in this study, we used *Pp6* conditional deletion in T_{reg} cells of ($Pp6^{fl/fl}$-$FoxP3^{GFP\text{-}cre}$, cKO) mice and determined the possible role of Pp6 in T_{reg} cell function and stability and depict the mechanisms. We showed that *Pp6* conditional knockout (cKO) in T_{reg} cells led to spontaneous autoinflammation in mice and diminished FoxP3 expression in T_{reg} cells. Loss of Pp6 in T_{reg} cells impaired their immunosuppressive function and exacerbated experimental colitis and EAE. Mechanistically, Pp6 deficiency increased CpG motif methylation of the FoxP3 locus by impairing the dephosphorylation of Dnmt1 and enhancing Akt signaling, leading to reduced FoxP3 in T_{reg} cells. We identified Pp6 as a critical positive regulator of FoxP3 that maintains T_{reg} cell stability and prevents autoimmune diseases.

Materials and methods

Mice

$Pp6^{fl/fl}$ mice bearing *loxP*-flanked exons 5—6 of the *Pp6* gene were hybridized with $FoxP3^{GFP\text{-}cre}$ mice to gain the specific cre-mediated deletion of *Pp6* in $FoxP3^+$ cells ($Pp6^{fl/fl}$-$FoxP3^{GFP\text{-}cre}$, cKO) mice. Genotype identification of the cKO mice by RT-PCR was shown in our previous paper.[10] The background of $FoxP3^{GFP\text{-}cre}$ mice was described as previous study[21,22] and the $FoxP3^{GFP\text{-}cre}$ mice were kindly provided

by Dr. Zhou Xuyu (Institute of Microbiology, Chinese Academy of Sciences, Shanghai, China). The background of *Pp6*$^{fl/fl}$ mice was described in previous study[23] and the *Pp6*$^{fl/fl}$ mice were kindly provided by Dr. Tao Wufan (National Center for International Research of Development and Disease, School of Life Sciences, Fudan University, Shanghai, China). *Rag1*$^{-/-}$ mice were obtained from the Model Animal Research Center of Nanjing University.

All *in vivo* and *in vitro* experiments were performed on 6- to 13-week-old mice. All mice were kept under specific pathogen-free (SPF) conditions in compliance with the National Institutes of Health Guide for the Care and Use of Laboratory Animals with the approval (SYXK-2018-0027) of the Scientific Investigation Board of Shanghai Jiaotong University School of Medicine. Mice used in disease models were euthanized by CO_2 inhalation when recommended to ameliorate any further suffering.

Cell culture

EL-4 cells were cultured in DMEM high glucose (HyClone) with 10% FBS and 1% penicillin/streptomycin. All cells were grown at 37 °C, 5% CO_2.

Flow cytometric analysis

Single-cell suspensions from mouse tissues were prepared in PBS containing 2% FBS. Cells were fixed and permeabilized with a Cytofix/Cytoperm kit (BD Biosciences) or FoxP3/Transcription Factor Staining Buffer Set (eBioscience). For surface marker analysis, cells were stained with the indicated antibodies (Abs) in PBS containing 2% FBS. Intracellular staining was performed according to the manufacturer's instructions. The following antibodies were used: anti-mouse CD4 APC-cy7, anti-mouse CD25 BV421/PE, anti-mouse FoxP3 APC, anti-mouse CD62L APC, anti-mouse CD44 PE, anti-mouse IFN-γ PE, anti-mouse IL-17A APC, anti-CD4 APC, and anti-Foxp3 PE from BioLegend. The anti-mouse/rat Ki67 was purchased from ebioscience. The anti-Akt-pSer473 rabbit antibody and anti-Akt-pThr308 rabbit antibody were purchased from Cell Signaling Technology as primary antibodies, and the donkey anti-rabbit AF594 secondary antibody was purchased from Invitrogen. Finally, the cells were washed, resuspended, and analyzed with a BD LSRFortessa X-20 flow cytometer.

ELISA

Quantitative analysis of IL-17A and IFN-γ in plasma of mouse was performed by ELISA using commercially available kits (Mouse IL-17A: Anogen, #MEC1001, mouse Interferon-Gamma (IFN-γ): Anogen, #MEC1002).

Histological analysis

The mouse tissue and organ samples were fixed in formalin and embedded in paraffin. Sections (6 μm) were stained with hematoxylin and eosin (H&E). Image analysis was performed using a Leica SP8 X confocal microscope.

Western blot analysis

Cells were directly lysed by RIPA lysis buffer (Beyotime) on ice, and proteins were separated by SDS-PAGE gels. Separated proteins were transferred to a PVDF membrane (Millipore), and the membrane was incubated for 1 h in TBS buffer (20 mM Tris—HCl pH 7.5, 500 mM NaCl) containing 5% BSA and 0.1% Tween 20 at room temperature. The membranes were incubated with primary antibody overnight at 4 °C and subsequently washed three times with TBS buffer containing 0.1% Tween 20. Then, the membranes were incubated with HRP secondary antibody for 1 h at room temperature. After washing and incubation with HRP substrate, signals were detected by an Amersham Imager 600 (GE). The following antibodies were used: anti-Pp6 (Millipore/Santa Cruz), anti-Akt (Cell Signaling Technology), anti-Akt-pSer473 (Cell Signaling Technology), anti-Akt-pThr308 (Cell Signaling Technology), anti-Actin (Beyotime), anti-pStat5 (Cell Signaling Technology), anti-FoxP3 (Abcam), anti-pJak3 (Cell Signaling Technology), anti-pSmand2/3 (Cell Signaling Technology), and anti-Smand2/3 (Abcam).

Induction of experimental allergic encephalomyelitis (EAE)

EAE was induced by complete Freund's adjuvant (CFA)-MOG_{35-55} peptide immunization (China Peptides Biotechnology) and scored daily. Briefly, cKO/control mice were injected subcutaneously into the base of the tail with a volume of 200 μl containing 300 μg MOG_{35-55} peptide emulsified in CFA (Sigma—Aldrich). Mice were also injected intravenously with 200 ng of pertussis toxin (Merck-Calbiochem) on days 0 and 2 postimmunization. All the reagents used for *in vivo* experiments were free of endotoxin. Mice were monitored daily for the development of disease, which was scored according to the following scale: 0, no symptoms; 0.5, partial limp tail; 1, complete limp tail; 2, the mouse was paralyzed in one hind limb; 3, both hind limbs were paralyzed, mouse drags hind limbs when crawling forward; 4, the mouse lost the use of both forelimbs, leaving the mouse immobile; 5, moribund and the body curled up; and 6, death.

Adaptor transfer

For adoptive transfer, freshly isolated $CD4^+$ $CD25^-$ $CD45RB^{hi}$ T cells from WT C57 mice and $CD4^+$ $CD25^+$ GFP^+ T_{reg} cells from *FoxP3*$^{GFP\text{-}cre}$ or cKO mice were obtained by FACS Sorting. *Rag1*$^{-/-}$ mice were coinjected with $CD4^+CD25^-CD45RB^{hi}$ T cells (5×10^5) and control/cKO nT_{reg} cells (2×10^5) *i.v.* and weighed every day.

T_{reg} cell induction

Mice were sacrificed, their spleens were removed and gently dissociated into single-cell suspensions. Naïve T cells were isolated using the MojoSort Mouse CD4 Naïve T Cell Isolation Kit (BioLegend). T cells were cultured in U-bottom 96-well plates with RPMI 1640 culture medium supplemented with 10% heat-inactivated fetal bovine serum (FBS;

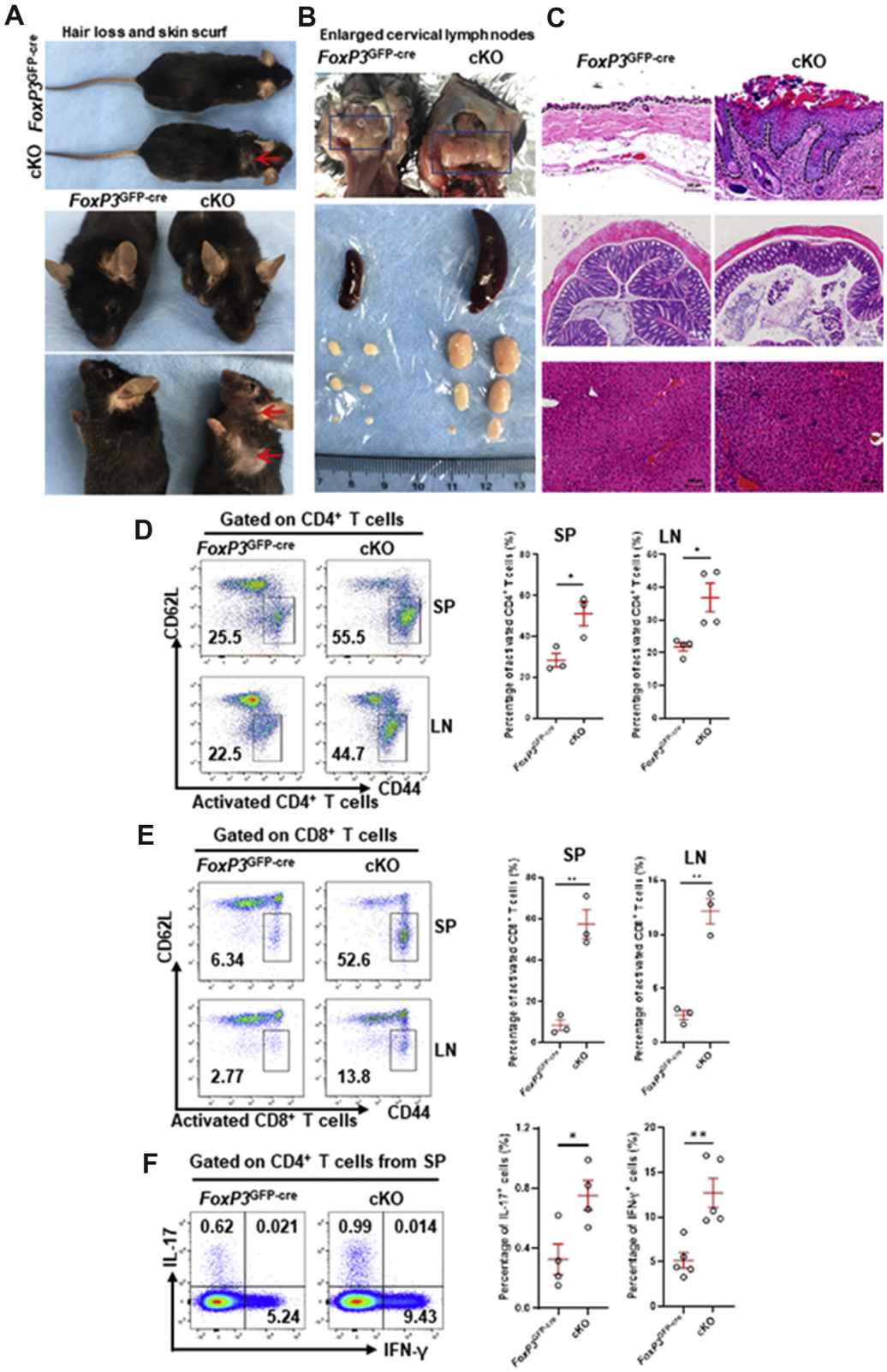

Figure 1 *Pp6*$^{fl/fl}$-*FoxP3*$^{GFP\text{-}cre}$ mice spontaneously develop autoimmunity and inflammation. Comparison of the *FoxP3*$^{GFP\text{-}cre}$ (control) mouse to the *Pp6*$^{fl/fl}$-*FoxP3*$^{GFP\text{-}cre}$ (cKO) mouse (three months of age). **(A)** Autoimmune signatures appeared in the cKO mouse. Hair loss and skin scurf are marked by red arrows. **(B)** The spleens and lymph nodes of cKO mice were significantly enlarged. Enlarged cervical lymph nodes are marked by blue boxes. **(C)** Representative hematoxylin and eosin (HE) staining of skin (*top*), colon (*middle*) and liver (*bottom*) sections from cKO/control mice. The dotted line indicates the border between the epidermis and the dermis; scale bar. Scar bars, 100 μm or 200 μm. Representative sections from four mice are shown. **(D—H)** Spleen (SP) or lymph

Gibco), 2 mM L-glutamine, 1% antibiotic-antimycotic (Gibco), 10 mM HEPES (Gibco), 1× nonessential amino acids (Gibco), 1 mM sodium pyruvate (Gibco), and 55 μM β-mercaptoethanol (Gibco). Naïve T cells were activated with plate-bound anti-CD3 (3 μg/ml; Bio X Cell) and soluble anti-CD28 (2 μg/ml; Bio X Cell) antibodies. T_{reg} cell differentiation was achieved by the indicated concentration of recombinant human TGF-β (R&D). The Akt inhibitor MK-2206 and afuresertib were purchased from MedChemExpress (MCE). Cells were cultured for 72 h and detected by flow cytometry.

Immunoprecipitation

To determine the interaction between Pp6 and Dnmt1 or Akt, EL-4 cells were lysed by RIPA buffer or WB-IP buffer (Beyotime). Equal amounts of lysates were incubated with protein A/G magnetic beads (Bimake) and antibodies, including Pp6 antibody (Millipore), Dnmt1 antibody (Abcam), or Akt antibody (Cell Signaling Technology). The prepared mixture was incubated overnight at 4 °C with agitation. The mixture was washed three times with PBS or lysis buffer and boiled in sample buffer. Then, the prepared immunoprecipitation complex was eluted for Western blot analysis to determine the interacting protein levels. Total cell protein was used as an input. The specificity of antibodies used for immunoprecipitation was routinely validated by using a negative control IgG.

Phos-tag SDS/PAGE

Briefly, for Mn^{2+} Phos-tag SDS/PAGE, 50 μM acrylamide-pendant Phos-tag ligand (APExBIO) and 100 μM $MnCl_2$ were added to a 6% separating gel before polymerization. Phos-tag SDS/PAGE was performed as described previously.[24]

Bisulfite sequencing PCR

Genomic DNA was denatured, modified with sodium metabisulfite, purified, and desulfonated. The FoxP3 upstream enhancer CpG motif located −5.7 kb from the TSS was PCR amplified using 5′-AATGTGGGTATTAGGTAAAATTTTT-3’ (forward) and 5′-AAACCCTAAAACTACCTCTAAC-3’ (reverse) primers. The TSDR located −2.5 kb from the CDS was PCR amplified using 5′-AGGAAGAGAAGGGGGTAGATA-3’ (forward) and 5′-AAACTAACATTCCAAAACCAAC-3’ (reverse) primers. PCR products were separated on agarose gels, excised, and cloned into the pGEM-T easy vector (Promega). Recombinant plasmid DNA from the individual bacterial colonies was purified and sequenced.

Statistics

The data were analyzed with GraphPad Prism 8 and are presented as the mean ± s.e.m. Student’s *t*-test was used when two conditions were compared, and analysis of variance (ANOVA) with Bonferroni or Newman−Keuls correction was used for multiple comparisons. Error bars indicate the mean ± s.e.m. $P < 0.05$ was considered statistically significant (ns = not significant, $^{*}P < 0.05$, $^{**}P < 0.01$, and $^{***}P < 0.001$).

Results

Mice with Pp6 conditional deletion in T_{reg} cells spontaneously develop autoimmunity

We previously reported that Pp6 is a critical regulator in the differentiation of T_{reg} cells that regulates Ang II-induced blood pressure elevation.[10] To investigate the role of Pp6 in T_{reg}-related autoimmune diseases, we generated mice with conditional *Pp6* knockout in T_{reg} cells (*Pp6*$^{fl/fl}$-*FoxP3*$^{GFP\text{-}cre}$, cKO) (Fig. S1A). Depletion of *Pp6* was confirmed with high efficiency in T_{reg} cells by Western blot (Fig. S1B). We compared cKO mice with FoxP3$^{GFP\text{-}cre}$ control mice, and found that cKO mice at 3 months of age developed inflammatory symptoms similar to scurfy mice (*FoxP3* mutant mice)[7]: hair loss in head and neck, thickening and roughening of skin, skin scurf, and acanthoid (Fig. 1A); considerably enlarged spleens and lymph nodes (Fig. 1B), increased inflammatory cell infiltration, and distinct inflammatory patterns in skin (*top*), colon (*middle*) and liver (*bottom*) by histological analysis (Fig. 1C). Together, these data suggest that specific deletion of *Pp6* in $CD4^{+}FoxP3^{+}$ T_{reg} cells leads to spontaneous autoinflammation.

Prompted by these autoinflammatory phenotypes, we further compared the activation state of immune cells derived from cKO mice and *FoxP3*$^{GFP\text{-}cre}$ control mice by flow cytometry. We found that the percentages of activated $CD4^{+}$ and $CD8^{+}$ T cells ($CD4^{+}$ $CD44^{hi}$ $CD62L^{low}$ T cells and $CD8^{+}$ $CD44^{hi}$ $CD62L^{low}$ T cells) were markedly increased in the spleens and lymph nodes of cKO mice (Fig. 1D, E), and the percentages of Th17 and Th1 cells were also elevated in the spleens of cKO group (Fig. 1F). We also examined the plasma level of pro-inflammatory cytokines IL-17A and IFN-γ by ELISA, and found cKO mice developing autoinflammation spontaneously have higher level of IL-17A, but no change of IFN-γ in plasma in comparison to control mice (Fig. 1G). Collectively, our data demonstrates that conditional ablation of *Pp6* in T_{reg} cells leads to the spontaneous development of autoimmunity and inflammation in mice.

node (LN) single-cell suspensions from cKO/control mice were probed by flow cytometry with the indicated antibodies. Representative flow cytometric analysis of CD62L and CD44, showing the activated $CD4^{+}$ T cell **(D)** and activated $CD8^{+}$ T cell **(E)** percentages after gating on $CD4^{+}$ T cells or $CD8^{+}$ T cells, respectively. Representative flow cytometric analysis of IL-17 and IFN-γ after gating on $CD4^{+}$ T cells, showing the proportion of Th1 and Th17 cells **(F)**. Data are representative of 3−4 independent experiments. Quantification of cells on the right. **(G)** Release of IL-17A and IFN-γ from the plasma of control/cKO mice. The plasma was recovered and the concentrations of IL-17A and IFN-γ were measured by enzyme-linked immunosorbent assay (ELISA). Data are presented as the mean ± s.e.m.of 6 independent experiments. $^{*}P < 0.05$, $^{**}P < 0.01$ by Student’s *t*-test. Error bars indicate the mean ± s.e.m.

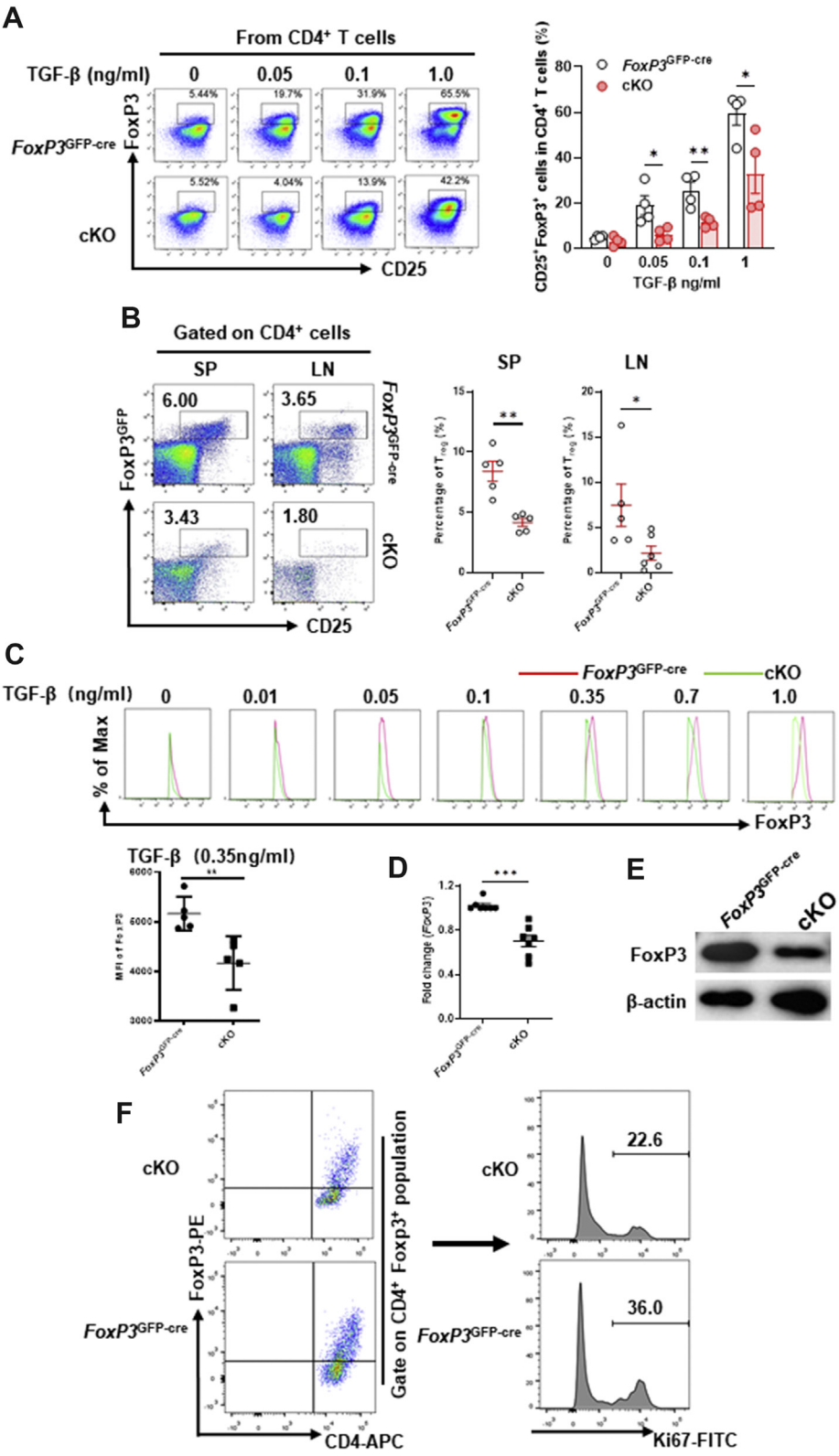

Figure 2 *Pp6* deficiency reduces FoxP3 expression in T_{reg} cells. Naïve $CD4^+$ T cells isolated from the spleen of cKO/control mice were induced to differentiate into T_{reg} (iT_{reg}) cells *in vitro* with different concentrations of TGF-β. Flow cytometric staining for CD25 and FoxP3 after gating on $CD4^+$ T cells; numbers in panels demonstrate the proportion of iT_{reg} cells ($CD4^+$ $CD25^+$ $FoxP3^+$) in each. Statistical chart showing the quantification of iT_{reg} cell percentages ($n = 4$). **(B)** Flow cytometric detection of CD25 and $FoxP3^{GFP}$ after gating on $CD4^+$ T cells, showing the proportion of nT_{reg} cells isolated from cKO/control mouse spleens and lymph nodes (statistical charts on the right). **(C—E)** The expression of FoxP3 in iT_{reg} cells derived from control and cKO mice was investigated by flow cytometric staining for FoxP3 after gating on $CD4^+CD25^+FoxP3^+$ T cells, statistical chart showing FoxP3 MFI at

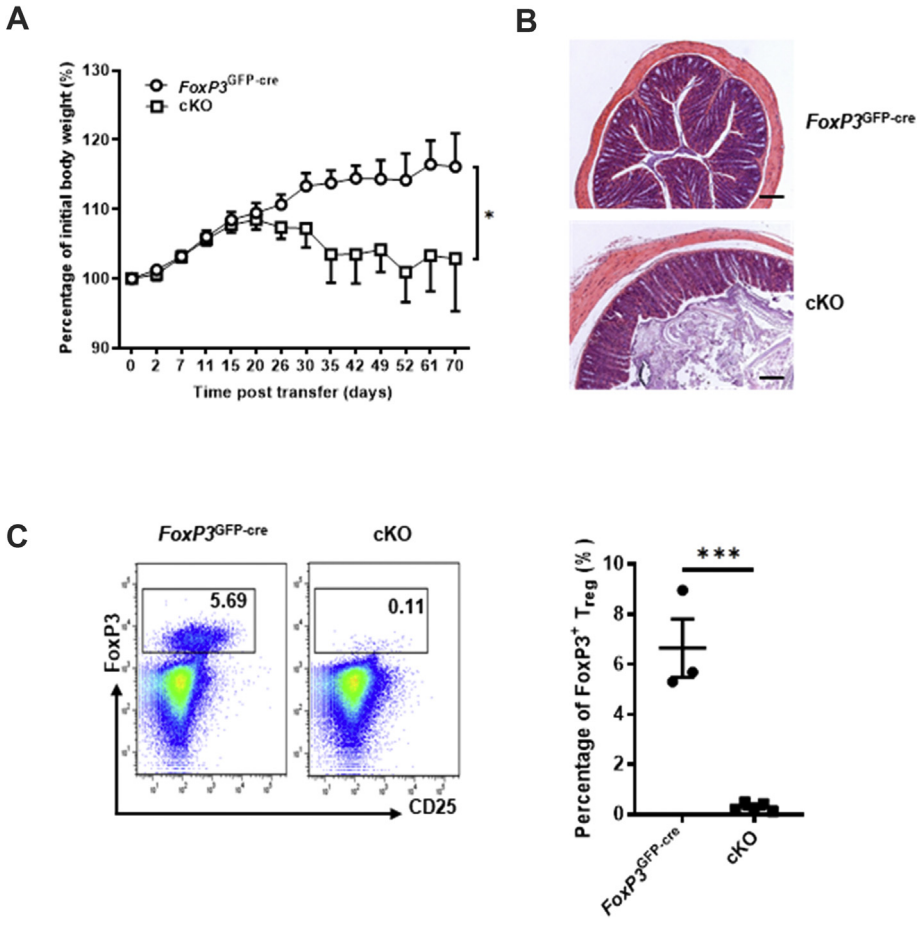

Figure 3 Impaired immunosuppressive function of *Pp6*$^{-/-}$ T_{reg} cells *in vivo*. We constructed an adoptive transfer colitis mouse model in *Rag1*$^{-/-}$ mice (coinjected naïve T cells isolated from C57 WT mice with T_{reg} cells sorted from either *FoxP3*$^{GFP\text{-}cre}$ control mice or cKO mice) and built two groups of mice: *FoxP3*$^{GFP\text{-}cre}$ and cKO. **(A)** Body weight changes of the above two groups of colitis model mice ($n = 10$). *$P < 0.05$ by Two-way ANOVA. **(B)** Representative H&E histology images of colons from the above two groups of colitis model mice on day 70 (bars represent 200 μm). Representative sections from six mice are shown. **(C)** Flow cytometric staining for CD25 and FoxP3 after gating on CD4$^+$ T cells, showing the proportion of T_{reg} cells from the spleen of the above two groups of colitis model mice on day 70. Statistical chart of the above two groups of colitis model mice showing the quantification of T_{reg} cell percentages ($n = 3$ or 5). ***$P < 0.001$ by Student's *t*-test. Error bars indicate the mean ± s.e.m.

Pp6 deficiency leads to diminished FoxP3 expression in T_{reg} cells

Next, we sought to better define the role of Pp6 as a modulator of T_{reg} cell development. First, we found that the lack of Pp6 markedly inhibited T_{reg} cell differentiation from naïve CD4$^+$ T cells of cKO mice compared with Foxp3$^{GFP-Cre}$ controls *in vitro* (Fig. 2A), which is consistent with our previous study.[10] Our *in vivo* results further demonstrated that cKO mice present a much lower proportion of natural T_{reg} (nT_{reg}) cells in the spleen and lymph nodes (Fig. 2B). Second, we investigated the expression of FoxP3 in iT_{reg} cells derived from control and cKO mice and found that FoxP3 protein levels in cKO iT_{reg} cells were lower than those in control iT_{reg} cells, and that this reduction was TGF-β concentration dependent (Fig. 2C). Moreover, both FoxP3 mRNA and protein levels were markedly decreased in cKO iT_{reg} cells (Fig. 2D, E). Third, we examined the proliferative function of iTreg cells derived from control and cKO mice by flow cytometry and found that Ki67 expression in cKO iT_{reg} cells (CD4$^+$ Foxp3$^+$ populations) were lower than those in control iT_{reg} cells (Fig. 2F). These results suggest that Pp6-deficient T_{reg} cells appear to have unstable expression of FoxP3 and strongly indicate that Pp6 is a critical regulator that maintains the stability of FoxP3 and the functional stability of T_{reg} cells.

0.35 ng/ml TGF-β concentration (**C**, $n = 3$–5), RT-PCR (**D**, $n = 7$), and Western blot (**E**, data are representative of three independent experiments). **(F)** The expression of Ki67 in iT_{reg} cells (CD4$^+$ Foxp3$^+$ populations) derived from control and cKO mice was investigated by flow cytometric staining for anti-CD4 APC, anti-Foxp3 PE and anti-Ki67 FITC after gating on CD4$^+$ FoxP3$^+$ T cells. *$P < 0.05$, **$P < 0.01$ by Student's *t*-test. Error bars the indicate mean ± s.e.m.

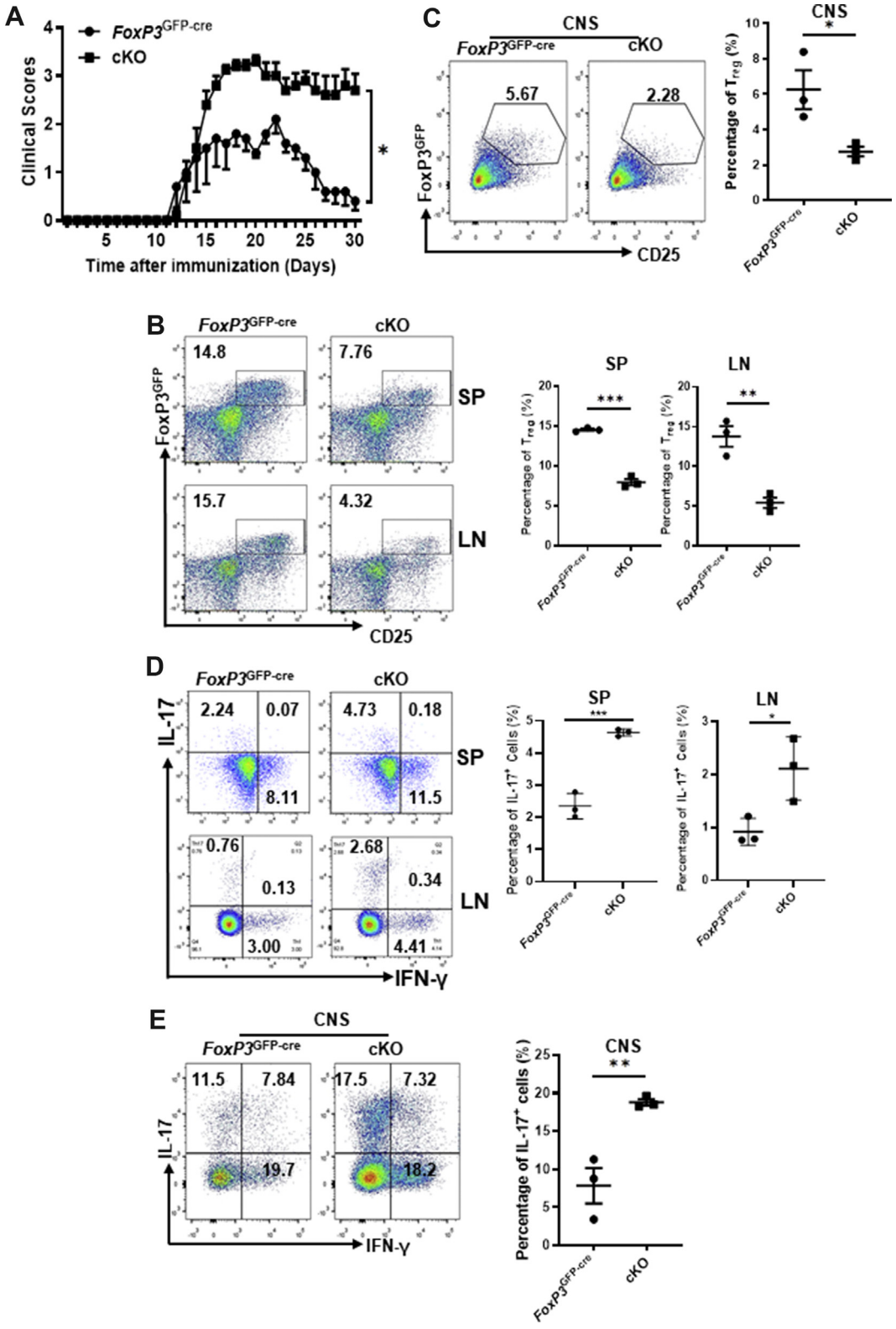

Figure 4 Loss of *Pp6* in T_{reg} cells exacerbates EAE. We constructed an EAE mouse model in cKO and *FoxP3*$^{GFP\text{-}cre}$ (control) mice for two groups: cKO and *FoxP3*$^{GFP\text{-}cre}$. **(A)** The clinical scores of cKO and *FoxP3*$^{GFP\text{-}cre}$ mice were investigated during the progression of mouse EAE ($n = 5$). *$P < 0.05$ by Two-way ANOVA. **(B, C)** Flow cytometric detection of CD25 and *FoxP3*^{GFP} after gating on $CD4^+$ T cells, showing the proportion of T_{reg} cells from the spleen (SP), lymph nodes (LN) **(B)** or central nervous system (CNS) **(C)** of the above two groups of EAE model mice. Statistical chart showing the quantification of T_{reg} cell percentages ($n = 3$). **(D, E)** Flow cytometric staining for IL-17 and IFN-γ after gating on $CD4^+$ T cells, showing the proportion of Th1 and Th17 cells from SP and LN **(D)**, CNS **(E)** of the above two groups EAE model mice. Statistical chart showing the quantification of Th17 and Th1 cell percentages ($n = 3$). *$P < 0.05$, **$P < 0.01$, ***$P < 0.001$ by Student's *t*-test. Error bars indicate the mean ± s.e.m.

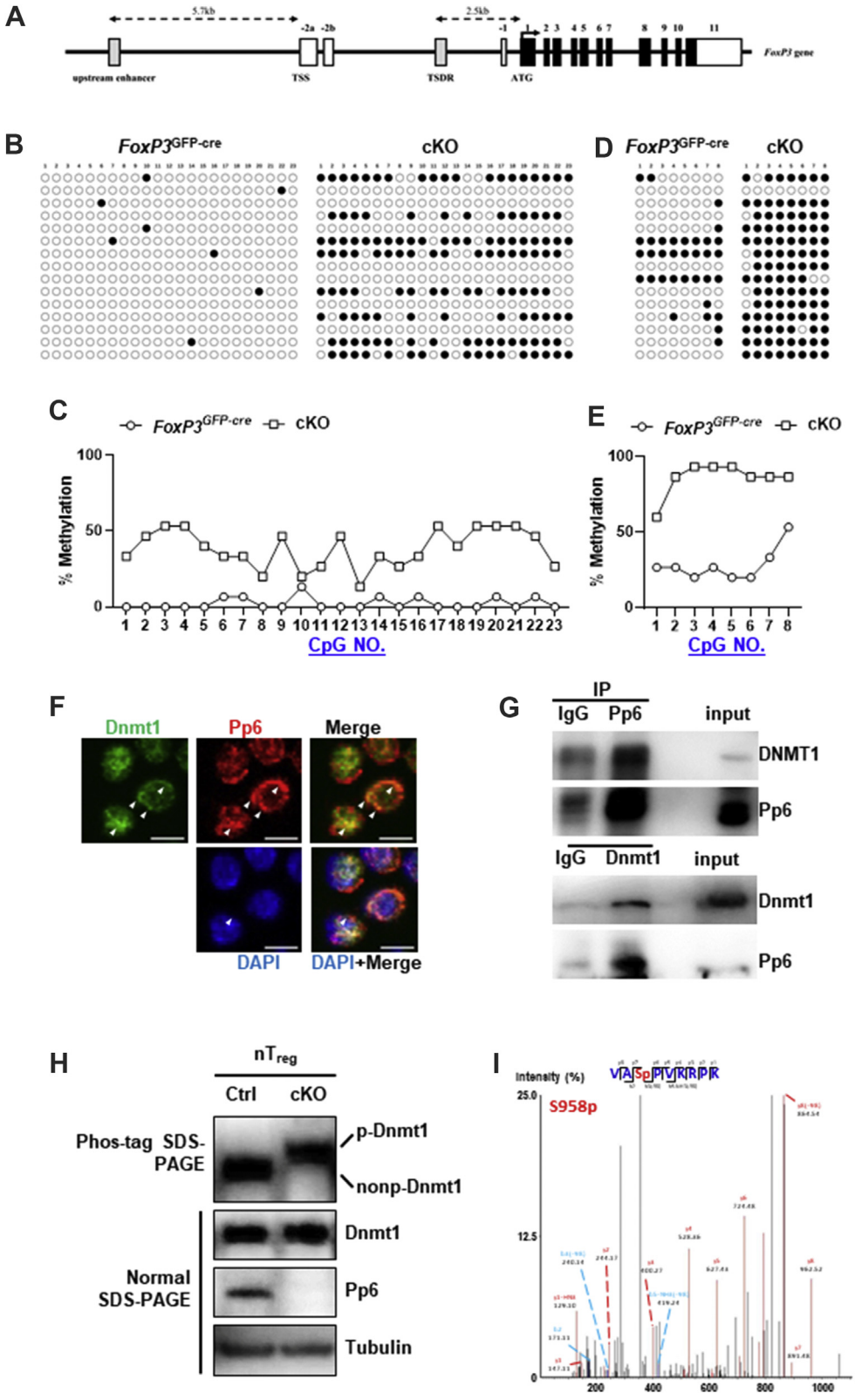

Figure 5 *Pp6* deficiency increased the CpG motif methylation of the *FoxP3* locus and bated the dephosphorylation of Dnmt1 in T_{reg} cells. **(A)** Schematic view of the *FoxP3* locus depicting the positioning of upstream enhancers and T_{reg}-specific demethylated regions (TSDRs). **(B)** Assessment of DNA methylation of the upstream *FoxP3* enhancer CpG island in cKO and *FoxP3*$^{GFP\text{-}cre}$ nT_{reg} cells was determined by bisulfite sequencing PCR (BSP). Open circles indicate demethylated CpG, and closed circles indicate methylated CpG. **(C)** Statistical chart showing the quantification of methylated CpG percentage for each site. **(D)** Assessment of TSDR DNA methylation in cKO and *FoxP3*$^{GFP\text{-}cre}$ nT_{reg} cells was determined by BSP. Open circles indicate demethylated CpG, and closed circles

Loss of Pp6 in Treg cells impairs their immunosuppressive function *in vivo* and exacerbates experimental colitis

Decreased FoxP3 levels indicate an impaired function of Treg cells. To evaluate whether the immunosuppression of *Pp6*$^{-/-}$ T_{reg} cells is disrupted in cKO mice, we established a mouse adoptive transfer colitis model. *Rag1*$^{-/-}$ mice that received WT naïve T cells and *Pp6*$^{-/-}$ T_{reg} cells had significant weight loss and colon tissue damage, while the adoptive transfer of control T_{reg} cells protected mice from colitis (Fig. 3A, B). Consistently, the numbers of FoxP3^{+} T_{reg} cells in the spleens of mice adoptively transferred with *Pp6*$^{-/-}$ T_{reg} cells were dramatically decreased at the end of this model (on day 70), suggesting that Pp6 is very important to maintaining the T_{reg} cell population (Fig. 3C). These data indicated that Pp6 deficiency in T_{reg} cells aggravated the colitis development induced by effector T cells and suffered from disabled T_{reg} cell immunosuppressive function.

Loss of Pp6 in T_{reg} cells exacerbates autoimmune disease

To further define the role of Pp6 in T_{reg}-related autoimmune disease, we took advantage of experimental allergic encephalomyelitis (EAE), a classical model of autoimmunity immunosuppressed by T_{reg} cells that is widely used to examine T_{reg} cell functions. EAE was established, and clinical manifestations started to appear on day 10 upon immunization in *FoxP3*$^{GFP\text{-}cre}$ and cKO mice. We found that the disease score of the cKO group was significantly higher than that of the control group (Fig. 4A). Furthermore, flow cytometry results showed that the CD25^{+} FoxP3^{+} T_{reg} cells decreased in the spleen, lymph nodes, and CNS of the cKO EAE model mice (Fig. 4B, C). Correspondingly, the proportion of Th17 cells in the above three organs of cKO mice was higher than that in the control group, while the proportion of Th1 cells remained unchanged (Fig. 4D, E). These results suggest that the development of T_{reg} cells in cKO mice is impaired and fails to inhibit the overactivated immune response mediated by effector T cells, eventually leading to a more severe EAE outcome.

Pp6 deficiency increased CpG motif methylation at the FoxP3 locus by impairing dephosphorylation of Dnmt1 in T_{reg} cells

Our data strongly suggest the instability of FoxP3 expression and fragility of T_{reg} cells in *Pp6* knockout mice. The transcriptional initiation of *FoxP3* is mediated by several signaling pathways, while CpG motif methylation of the *FoxP3* locus controls the stability of FoxP3 expression.[25] To elucidate the mechanism, we investigated the level of CpG motif methylation of the *FoxP3* locus in cKO T_{reg} cells. We analyzed the methylation levels of canonical and noncanonical CpG motifs by bisulfite sequencing PCR (BSP). Specifically, the *FoxP3* upstream enhancer is located −5.7 kb from the TSS, containing 23 CpGs as the noncanonical CpG motif, and the T_{reg}-specific demethylated region (TSDR) is located −2.5 kb from the CDS, containing 8 CpGs as the canonical CpG motif (Fig. 5A). In WT mice, both CpG motifs are methylated in naïve T cells and effector T cells but demethylated in nT_{reg} cells.[26,27] In contrast, we found that the DNA methylation of CpG in the upstream enhancer and TSDR were both increased in cKO nT_{reg} cells (Fig. 5B–E).

To determine how Pp6 modulates CpG motif methylation of *FoxP3* locus events, we first looked for Pp6 binding proteins by immunoprecipitating overexpressed Pp6 in the mass spectrum and found a Pp6 binding candidate, Dnmt1 (Fig. S3A), which is an enzyme for DNA methylation and has been considered an critical factor for T_{reg} cell development.[14,27] To verify Dnmt1 as a substrate of Pp6 and confirm their interactions *in vivo*, we first immunostained endogenous Dnmt1 and Pp6 in CD4^{+} T cells and detected the signals by confocal microscopy. As expected, Dnmt1 (*green*) and Pp6 (*red*) were frequently colocalized in both the cytoplasm and nuclei, as shown in merged images (*yellow*) (Fig. 5F). Second, for the protein–protein interaction, we immunoprecipitated Pp6 or Dnmt1 from EL-4 cell lysates and then detected both endogenous *Pp6*/*Pp6* and Dnmt1/Dnmt1 by Western blot (Fig. 5G). Together, these results demonstrate that Pp6 colocalized and directly interacted with Dnmt1. Third, we detected Dnmt1 phosphorylation in Ctrl/cKO nT_{reg} cell lysates using the Phos-tag SDS-PAGE system, which could shift the phosphorylated protein above the nonphosphorylated protein in the gel. The results clearly showed that Dnmt1 was phosphorylated in cKO cells compared to control cells (Fig. 5H). To further identify the specific phosphorylation site of Dnmt1, we identified by mass spectrometry that Ser958 was the phosphorylation site of Dnmt1 in EL-4 T cells (Fig. 5I). Interestingly, pSer958 is in a p-serine-proline sequence, a motif reported as a proline-directed (phospho-Ser-Pro) dephosphorylation site of Pp6.[28] In homology analysis, the nearby protein sequence of Ser958 shows high homology among humans, mice, rats, bovines, chickens, and zebrafish, especially Ser958 and Pro959, which are in the Pp6 dephosphorylation site motif (Fig. 3B). These results indicate that pSer958 is an important phosphorylation site of Dnmt1 in T cells and is highly likely to be the dephosphorylation site of Pp6.

Together, our data shows that Pp6 probably dephosphorylates Dnmt1 in T_{reg} cells and impairs CpG motif

indicate methylated CpG. **(E)** Statistical chart showing the quantification of methylated CpG percentage for each site. **(F)** CD4^{+} T cells isolated from WT mouse spleens were fixed and immunostained with Pp6 (*red*), Dnmt1 (*green*) and DAPI (*blue*). Colocalized Pp6 and Dnmt1 were displayed in merge (*yellow*) by confocal microscopy. The bar represents 5 μm. **(G)** Cell lysates from EL-4 cells were subjected to immunoprecipitation (IP) using anti-Pp6 or anti-Dnmt1 antibodies, followed by immunoblotting with anti-Pp6 or anti-Dnmt1 antibodies, respectively. **(H)** nT_{reg} cells isolated from cKO and FoxP3GFP-cre (Ctrl) mice were lysed and analyzed by Phos-tag SDS-PAGE and normal SDS-PAGE Western blot. The blots were probed with antibodies against Pp6, Dnmt1 and tubulin. **(I)** The mass spectrum data show the phosphorylation site of the Dnmt1 protein extracted from EL-4 cells.

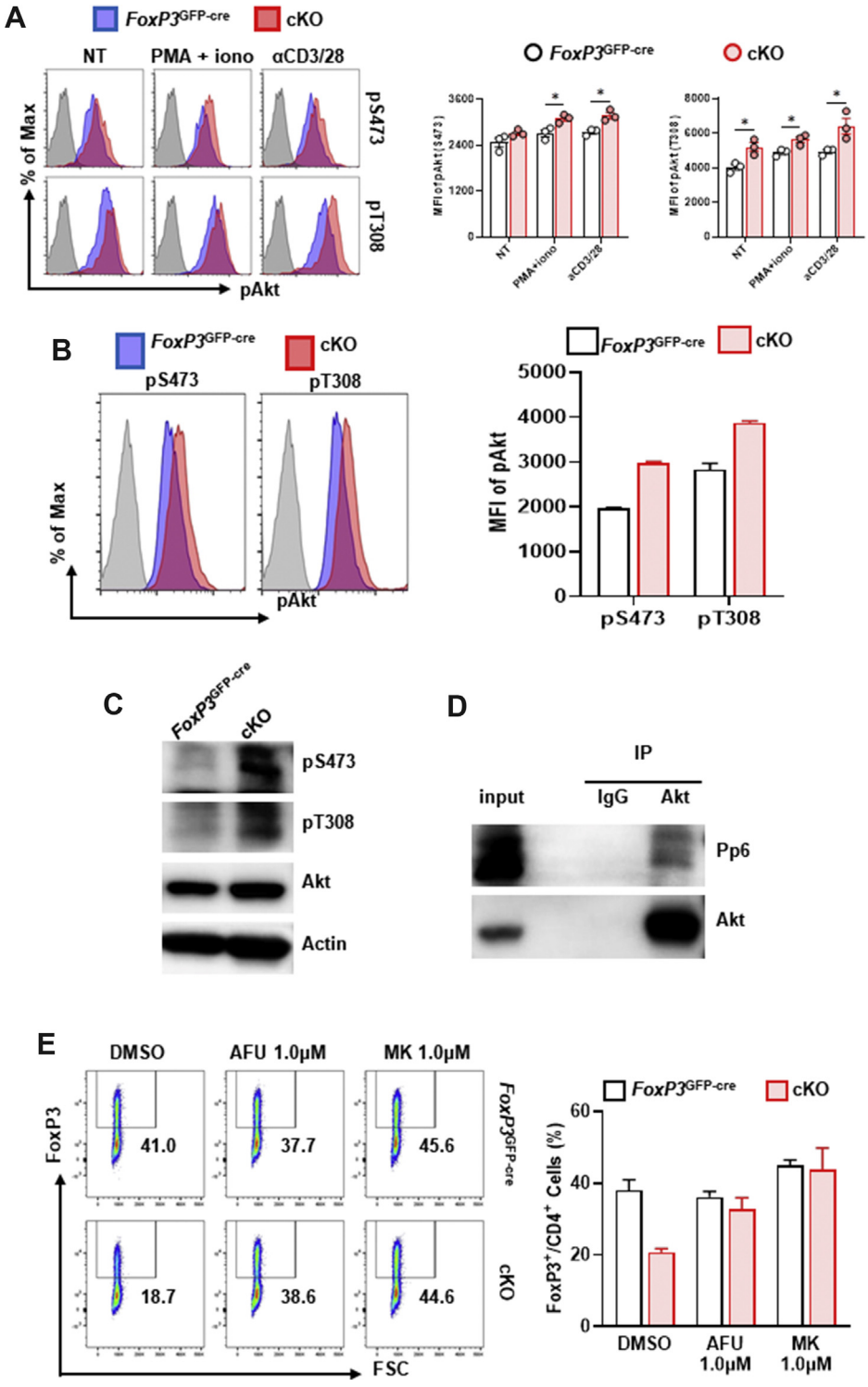

Figure 6 Loss of *Pp6* enhances Akt signaling, leading to impaired FoxP3 in T_{reg} cells. **(A)** Representative histograms of phosphorylation levels of pAKT-S473 and T308 after gating on FoxP3$^+$ CD4$^+$ T cells from cKO or control mouse spleens under different activation conditions; Iono (ionomycin), αCD3/28 (anti-CD3 and anti-CD28 antibodies). Statistical charts on the right, $n = 3$. **(B, C)** Naïve CD4$^+$ T cells isolated from the spleen of cKO/control mice were induced to differentiate into T_{reg} (iT_{reg}) cells *in vitro*. The phosphorylation levels of pAKT-S473 and T308 in iT_{reg} cells were measured by flow cytometry after gating on FoxP3$^+$ CD4$^+$ T cells **(B)** and Western blot **(C)**, statistical chart on the right. **(D)** Endogenous immunoprecipitation was performed using an anti-Akt antibody from EL-4 cells, followed by immunoblotting with anti-Pp6 or anti-Akt antibodies. **(E)** iT_{reg} cells from cKO/control mice were treated with DMSO, afuresertib (AFU) or MK-2206 (MK). Flow cytometric detection of FoxP3 after gating on CD4$^+$ T cells. Statistical chart showing the proportion of iT_{reg} cells. Data are representative of two independent experiments. *$P < 0.05$ by Student's *t*-test. Error bars indicate the mean ± s.e.m.

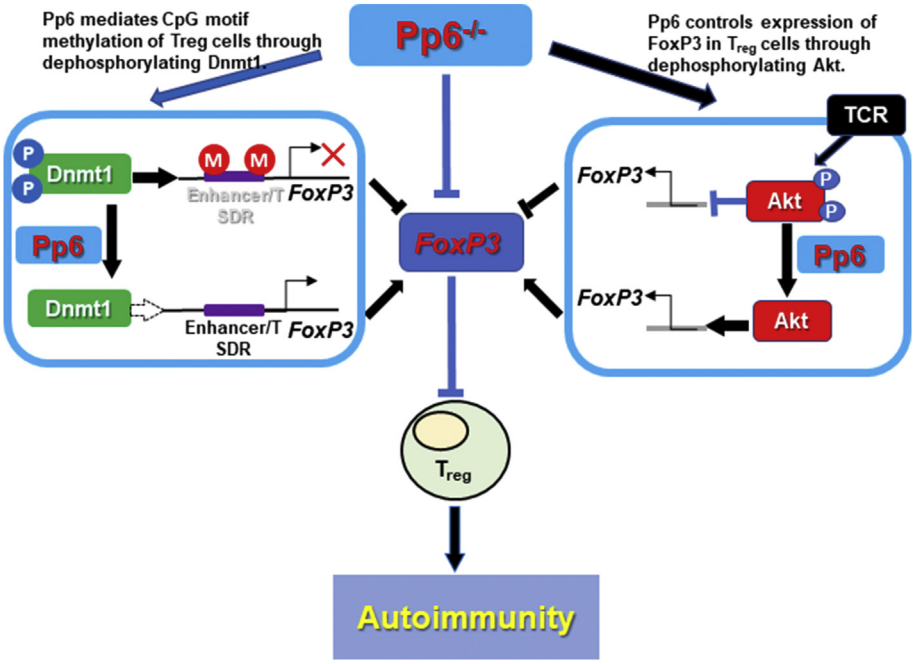

Figure 7 Scheme for Pp6 as a critical positive regulator of FoxP3 that dephosphorylates Dnmt1 and inhibits Akt signaling to maintain Treg cell stability and prevent autoimmunity. Pp6 decreased DNA methylation of the FoxP3 gene enhancer and Treg-specific demethylated region (TSDR) by dephosphorylating Dnmt1, resulting in increased FoxP3, and Pp6 abated phosphorylation of Akt, leading to enhanced FoxP3 in Treg cells.

methylation of the *FoxP3* locus, which leads to stable expression of FoxP3 and functional T_{reg} cell development. Ultimately, these actions balance the immune system and avoids autoimmunity development.

Loss of Pp6 enhances Akt signaling, leading to diminished levels of FoxP3 in T_{reg} cells

FoxP3 is inhibited by the Akt pathway, which is a key event for T_{reg} cell stability.[18,37] Therefore, we assessed phosphorylated Akt at S473 and T308 by flow cytometry in FoxP3$^+$ CD4$^+$ T_{reg} cells from control/cKO mouse spleens. Under stimulation with PMA/ionomycin or anti-CD3/CD28, both pS473 and pT308 were significantly increased (Fig. 6A). Consistently, FoxP3$^+$ CD4$^+$ cKO iT_{reg} cells displayed hyperactivated Akt at pS473 and pT308 compared with the control group (Fig. 6B, D). Furthermore, we detected an endogenous interaction between Akt and Pp6 by Western blot in the EL-4 mouse T cell line (Fig. 6C). To confirm whether the effect of Pp6 in T_{reg} cells depends on Akt activation, we used two kinds of inhibitors of Akt (afuresertib [AFU] and MK-2206 [MK])[29,30] to treat iT_{reg} cells *in vitro* and found that inhibition of Akt rescued the iT_{reg} cell proportion in the cKO group to the same level as that in the control group (approximately 20%—40%). Conversely, iT_{reg} cells in the control group showed no difference from Akt inhibitor treatment (Fig. 6E), indicating an inactivated Akt signal in normal T_{reg} cells. Here, we demonstrate that Pp6 is able to restrict Akt phosphorylation and that Pp6 deficiency impairs FoxP3 expression through excessive Akt signaling.

Collectively, our data shows that Pp6 diminishes pAkt at S473 and T308 in T_{reg} cells, which maintains FoxP3 expression and functional T_{reg} cell development. Pp6 is a critical factor that balances the immune system and prevents the development of autoimmunity.

Discussion

In this study, using mice with conditional *Pp6* deletion in T_{reg} cells, we showed that Pp6 is an essential positive regulator of FoxP3, maintains T_{reg} cell stability and prevents autoimmune diseases by decreasing DNA methylation of the FoxP3 gene enhancer and inhibiting Akt signaling (Fig. 7).

Both FoxP3 expression and establishment of a T_{reg} cell-specific hypomethylation pattern are indispensable for T_{reg} cell stability and function.[31] DNA methylation is generally catalyzed by one or more DNA methyltransferase (Dnmt) enzymes: Dnmt1, Dnmt3a, and Dnmt3b. Among them, Dnmt1 binds preferentially to hemimethylated DNA and re-establishes DNA methylation after its replication.[32] Ablation of Dnmt1, but not Dnmt3a, decreased the numbers and function of peripheral T_{reg} cells *in vivo* and impaired the conversion of naïve T cells to FoxP3$^+$ T_{reg} cells *in vitro*.[14] More importantly, mice with conditional knockout of Dnmt1 in FoxP3$^+$ T_{reg} cells died of autoimmunity by 3—4 weeks of age unless they were rescued by perinatal transfer of WT T_{reg} cells.[14] These published data highlight that Dnmt1 is a critical regulator of FoxP3$^+$ T_{reg} cell development, stability, and function.

Kinase and phosphatase are the Yin and Yang proteins modified via phosphorylation and dephosphorylation. The human genome encodes 518 protein kinases but only approximately 200 phosphatases (approximately 30 protein serine/threonine phosphatases).[33,34] Researchers generally

pay more attention to protein kinases than protein phosphatases and consider the dephosphorylation of protein phosphatases to be a nonspecific physiological function. However, phosphatases also have a wide range of important functions, such as in the cell cycle, inflammation, immune response, DNA repair, cancer, and almost all physiological processes.[9] In this study, we identified Pp6 as a critical protein phosphatase that dephosphorylates Dnmt1 in T_{reg} cells and impairs CpG motif methylation of the *FoxP3* locus, leading to stable expression of FoxP3 and functional T_{reg} cell development. We previously reported that activation of the NF-κB signaling pathway is responsible for decreased expression levels of Pp6 in chronic inflammation[35]; targeted therapy to maintain Pp6 expression therefore harbors therapeutic potential for autoimmune diseases.

TCR signaling and constitutive Akt activation antagonize FoxP3 induction.[36] Compared with kinases, research on phosphatases involved in Akt dephosphorylation is limited. PHLPP1/2 were reported to dephosphorylate Akt at Ser473 but not at Thr308,[18,38] and PP2A is mainly responsible for mTOC1 dephosphorylation.[19,20] Very interestingly, we demonstrated here that Pp6 directly interacts with Akt, and *Pp6* knockout dramatically elevates the phosphorylation of Akt at Ser473 and Thr308, which strongly suggests that Pp6 is able to dephosphorylate pAkt at Ser473 and Thr308. Our findings prove the importance of Pp6 in Akt signaling mediation and reveal the network of the PI3K-Akt-mTOR pathway in T_{reg} cells. Given that the PI3K-Akt-mTOR signaling network regulates FoxP3 expression and Pp6 is able to stabilize FoxP3, we suggest that Pp6 agonists could be considered for the treatment of autoimmune diseases or transplant rejection therapy. Conversely, Pp6 antagonists would also have potential benefits in antitumor immunotherapy.

In contrast to the TGF-β signaling pathway, which acts as an on/off switch, the methylation of the TSDR is generally reported to stabilize FoxP3 expression,[25] but its regulation is not clear. In our study, compared with control T_{reg} cells, *Pp6*-deficient T_{reg} cells had enhanced DNA methylation of the upstream enhancer and TSDR, which is an unstable epigenetic state for T_{reg} cells associated with T_{reg} cell plasticity. However, Akt signaling was reported to have a negative role in DNA methylation mediation.[39] Thus, our data indicate that the Akt signal is not responsible for the increased DNA methylation of the *FoxP3* locus in *Pp6*-deficient T_{reg} cells. Nevertheless, we found that Pp6 dephosphorylates Dnmt1 and impairs CpG motif methylation at the *FoxP3* locus, stabilizing FoxP3 expression in T_{reg} cells. The detailed regulatory network of Pp6, Akt, and Dnmt1 requires further investigation.

In conclusion, our results suggest that Pp6 decreased DNA methylation of the FoxP3 gene enhancer and abated phosphorylation of Akt, leading to stable expression of FoxP3 in T_{reg} cells. Therefore, Pp6 may be a potential therapeutic target for the treatment of autoimmune diseases.

Author contributions

W.C., (Wei CAI) and J.Z., (Junxun ZHANG) (First authors), H.W., (Honglin WANG) and Q.L. (Qun LI) (Corresponding authors) designed the project, W.C., J.Z., H.Z., XX.L., and F.L. performed the experiments; Y.S., Z.X., J.B., Q.Y., Z.W., L.S., X.C., S.T., Y.W., L.F., H.W., and Q.L. analyzed the data, J.Z., Q.L., and H.W. wrote the manuscript, Q.L., and H.W. supervised the study. All authors reviewed the results and approved the final version of the manuscript.

Conflict of interests

The authors declare that there are no conflicts of interest.

Funding

This work is supported by grants from the National Natural Science Foundation of China (No. 82070509, 81930088, 81725018), Innovative Research Team of High-Level Local Universities in Shanghai, and the Natural Science Foundation of Shanghai Science and Technology Committee, China (No. 20ZR1447400).

Acknowledgements

We thank Dr. ZHOU Xuyu (Institute of Microbiology, Chinese Academy of Sciences, Shanghai, China) for kindly providing *FoxP3*$^{GFP\text{-}cre}$ mice. We thank Dr. TAO Wufan (National Center for International Research of Development and Disease, School of Life Sciences, Fudan University, Shanghai, China) for kindly providing *Pp6*$^{fl/fl}$ mice.

Appendix A. Supplementary data

Supplementary data to this article can be found online at https://doi.org/10.1016/j.gendis.2021.07.005.

References

1. Pompura SL, Dominguez-Villar M. The PI3K/AKT signaling pathway in regulatory T-cell development, stability, and function. *J Leukoc Biol*. 2018;103:1065–1076.
2. Schallenberg S, Tsai PY, Riewaldt J, Kretschmer K. Identification of an immediate Foxp3(-) precursor to Foxp3(+) regulatory T cells in peripheral lymphoid organs of nonmanipulated mice. *J Exp Med*. 2010;207(7):1393–1407.
3. Zhou X, Bailey-Bucktrout SL, Jeker LT, et al. Instability of the transcription factor Foxp3 leads to the generation of pathogenic memory T cells in vivo. *Nat Immunol*. 2009;10(9):1000–1007.
4. Bailey-Bucktrout SL, Bluestone JA. Regulatory T cells: stability revisited. *Trends Immunol*. 2011;32(7):301–306.
5. Wing JB, Tanaka A, Sakaguchi S. Human FOXP3(+) regulatory T cell heterogeneity and function in autoimmunity and cancer. *Immunity*. 2019;50(2):302–316.
6. Li Z, Li D, Tsun A, Li B. FOXP3+ regulatory T cells and their functional regulation. *Cell Mol Immunol*. 2015;12(5):558–565.
7. Yilmaz OK, Haeberle S, Zhang M, Fritzler MJ, Enk AH, Hadaschik EN. Scurfy mice develop features of connective tissue disease overlap syndrome and mixed connective tissue disease in the absence of regulatory T cells. *Front Immunol*. 2019;10:881.
8. Wildin RS, Ramsdell F, Peake J, et al. X-linked neonatal diabetes mellitus, enteropathy and endocrinopathy syndrome is

the human equivalent of mouse scurfy. *Nat Genet*. 2001;27(1):18—20.
9. Ohama T. The multiple functions of protein phosphatase 6. *Biochim Biophys Acta Mol Cell Res*. 2019;1866(1):74—82.
10. Li X, Cai W, Xi W, et al. MicroRNA-31 regulates immunosuppression in Ang II (Angiotensin II)-induced hypertension by targeting Ppp6C (protein phosphatase 6c). *Hypertension*. 2019;73(5):e14—e24.
11. Polansky JK, Kretschmer K, Freyer J, et al. DNA methylation controls Foxp3 gene expression. *Eur J Immunol*. 2008;38(6):1654—1663.
12. Hori S. Developmental plasticity of Foxp3+ regulatory T cells. *Curr Opin Immunol*. 2010;22(5):575—582.
13. Chen ZX, Riggs AD. DNA methylation and demethylation in mammals. *J Biol Chem*. 2011;286(21):18347—18353.
14. Wang L, Liu Y, Beier UH, et al. Foxp3+ T-regulatory cells require DNA methyltransferase 1 expression to prevent development of lethal autoimmunity. *Blood*. 2013;121(18):3631—3639.
15. Li C, Ebert PJ, Li QJ. T cell receptor (TCR) and transforming growth factor β (TGF-β) signaling converge on DNA (cytosine-5)-methyltransferase to control forkhead box protein 3 (foxp3) locus methylation and inducible regulatory T cell differentiation. *J Biol Chem*. 2013;288(26):19127—19139.
16. Xia Q, Zhang J, Han Y, et al. Epigenetic regulation of regulatory T cells in patients with abdominal aortic aneurysm. *FEBS Open Bio*. 2019;9(6):1137—1143.
17. Garg G, Muschaweckh A, Moreno H, et al. Blimp1 prevents methylation of Foxp3 and loss of regulatory T cell identity at sites of inflammation. *Cell Rep*. 2019;26(7):1854—1868.
18. Liu Y, Xu Y, Sun J, et al. AKT hyperactivation confers a Th1 phenotype in thymic Treg cells deficient in TGF-β receptor II signaling. *Eur J Immunol*. 2014;44(2):521—532.
19. Apostolidis SA, Rodríguez-Rodríguez N, Suárez-Fueyo A, et al. Phosphatase PP2A is requisite for the function of regulatory T cells. *Nat Immunol*. 2016;17(5):556—564.
20. Kasper IR, Apostolidis SA, Sharabi A, Tsokos GC. Empowering regulatory T cells in autoimmunity. *Trends Mol Med*. 2016;22(9):784—797.
21. Lee EC, Yu D, Martinez de Velasco J, et al. A highly efficient Escherichia coli-based chromosome engineering system adapted for recombinogenic targeting and subcloning of BAC DNA. *Genomics*. 2001;73(1):56—65.
22. Zhou X, Jeker LT, Fife BT, et al. Selective miRNA disruption in T reg cells leads to uncontrolled autoimmunity. *J Exp Med*. 2008;205(9):1983—1991.
23. Ye J, Shi H, Shen Y, et al. PP6 controls T cell development and homeostasis by negatively regulating distal TCR signaling. *J Immunol*. 2015;194(4):1654—1664.
24. Sugiyama Y, Hatano N, Sueyoshi N, et al. The DNA-binding activity of mouse DNA methyltransferase 1 is regulated by phosphorylation with casein kinase 1delta/epsilon. *Biochem J*. 2010;427(3):489—497.
25. Huehn J, Polansky JK, Hamann A. Epigenetic control of FOXP3 expression: the key to a stable regulatory T-cell lineage? *Nat Rev Immunol*. 2009;9(2):83—89.
26. Floess S, Freyer J, Siewert C, et al. Epigenetic control of the foxp3 locus in regulatory T cells. *PLoS Biol*. 2007;5(2):e38.
27. Lal G, Zhang N, van der Touw W, et al. Epigenetic regulation of Foxp3 expression in regulatory T cells by DNA methylation. *J Immunol*. 2009;182(1):259—273.
28. Rusin SF, Schlosser KA, Adamo ME, Kettenbach AN. Quantitative phosphoproteomics reveals new roles for the protein phosphatase PP6 in mitotic cells. *Sci Signal*. 2015;8(398):rs12.
29. Manzella G, Schreck LD, Breunis WB, et al. Phenotypic profiling with a living biobank of primary rhabdomyosarcoma unravels disease heterogeneity and AKT sensitivity. *Nat Commun*. 2020;11(1):4629.
30. Cheng Y, Ren X, Zhang Y, et al. eEF-2 kinase dictates cross-talk between autophagy and apoptosis induced by Akt Inhibition, thereby modulating cytotoxicity of novel Akt inhibitor MK-2206. *Cancer Res*. 2011;71(7):2654—2663.
31. Ohkura N, Kitagawa Y, Sakaguchi S. Development and maintenance of regulatory T cells. *Immunity*. 2013;38(3):414—423.
32. He XJ, Chen T, Zhu JK. Regulation and function of DNA methylation in plants and animals. *Cell Res*. 2011;21(3):442—465.
33. Sacco F, Perfetto L, Castagnoli L, Cesareni G. The human phosphatase interactome: an intricate family portrait. *FEBS Lett*. 2012;586(17):2732—2739.
34. Hunter T. Protein kinases and phosphatases: the yin and yang of protein phosphorylation and signaling. *Cell*. 1995;80(2):225—236.
35. Yan S, Xu Z, Lou F, et al. NF-κB-induced microRNA-31 promotes epidermal hyperplasia by repressing protein phosphatase 6 in psoriasis. *Nat Commun*. 2015;6:7652.
36. Sauer S, Bruno L, Hertweck A, et al. T cell receptor signaling controls Foxp3 expression via PI3K, Akt, and mTOR. *Proc Natl Acad Sci U S A*. 2008;105(22):7797—7802.
37. Brognard J, Sierecki E, Gao T, Newton AC. PHLPP and a second isoform, PHLPP2, differentially attenuate the amplitude of Akt signaling by regulating distinct Akt isoforms. *Mol Cell*. 2007;25(6):917—931.
38. Patterson SJ, Han JM, Garcia R, et al. Cutting edge: PHLPP regulates the development, function, and molecular signaling pathways of regulatory T cells. *J Immunol*. 2011;186(10):5533—5537.
39. Zhang X, He X, Li Q, et al. PI3K/AKT/mTOR signaling mediates valproic acid-induced neuronal differentiation of neural stem cells through epigenetic modifications. *Stem Cell Reports*. 2017;8(5):1256—1269.